Hyperspectral image denoising and anomaly detection based on low-rank and sparse representations

Lina Zhuang[1], Lianru Gao[2], Bing Zhang[2] and José M. Bioucas-Dias[1]
[1]Instituto de Telecomunicações, Instituto Superior Técnico, Universidade de Lisboa, 1049-001, Lisbon, Portugal.
[2]Institute of Remote Sensing and Digital Earth, Chinese Academy of Sciences, Beijing, 100094, China.
Email: {lina.zhuang, bioucas}@lx.it.pt and {gaolr, zb}@radi.ac.cn

***Abstract*—The very high spectral resolution of Hyperspectral Images (HSIs) enables the identification of materials with subtle differences and the extraction subpixel information. However, the increasing of spectral resolution often implies an increasing in the noise linked with the image formation process. This degradation mechanism limits the quality of extracted information and its potential applications. Since HSIs represent natural scenes and their spectral channels are highly correlated, they are characterized by a high level of self-similarity and are well approximated by low-rank representations. These characteristic underlies the state-of-the-art in HSI denoising. However, in presence of rare pixels, the denoising performance of those methods is not optimal and, in addition, it may compromise the future detection of the rare pixels. To address these hurdles, we propose a powerful HSI denoiser which implements hard low-rank representation, promotes self-similarity in the representation coefficients, and, by using a form of collaborative sparsity, preserves rare pixels. The denoising and detection effectiveness of the proposed robust HSI denoiser is illustrated using semi-real data.**

I. Introduction

A. Background

HSIs have been widely used in countless applications, (e.g., earth observation, environmental protection and natural disaster monitoring), since they provide remarkably high spectral resolution (hundreds or thousands of spectral channels), which enables material identification with precision via spectroscopic analysis. However, the measurement noise often precludes the widespread use of HSIs in precise material identification (e.g., precision farming) applications.

Among the recent developments, low-rank and self-similarity based image denoising holds the state-of-the-art in HSI denoising (e.g., NAILRMA [1] and FastHyDe [2]). However, the presence of rare pixels, which are anomalies whose spectral-spatial characteristics are different from majority of pixels (often called background), degrade the denoising performance and may preclude the future detection of the rare pixels, called anomaly detection problem [3].

This work aims at endowing our previous FastHyDe denoiser [2] with the ability to preserve of rare pixels. We exploit three characteristics of HSIs: a) they are well approximated by low dimensional subspaces, b) their images of subspace representation coefficients, herein termed eigen-images, are self-similar and thus suitable to be denoised with non-local patch-based methods, such as the BM3D [4] or LRCF [5], and c) anomalies are often spatially sparse.

B. Observation Model

Assume that the dataset contains a small number of spectral or spatial outliers in unknown positions. The outliers are usually rare pixels or pixel corruptions due to malfunction of the sensor. In a way similar to robust PCA [6] and to the formulations [1], we adopt the observation model

$$\mathbf{Y} = \mathbf{X} + \mathbf{S} + \mathbf{N}, \tag{1}$$

which assumes that the observed data matrix $\mathbf{Y} \in \mathbb{R}^{n_b \times n}$ (whose n columns represent spectral vectors and n_b rows spectral bands) can be decomposed into three additive matrices of size $\mathbb{R}^{n_b \times n}$; given $\mathbf{Y}$, our objective is the estimation of $\mathbf{X}$ and $\mathbf{S}$, by exploiting the fact that $\mathbf{X}$ is low-rank and self-similar and $\mathbf{S}$ is columnwise sparse. This reasoning is similar to the robust principle component analysis [6]. The main difference with respect to (w.r.t) robust PCA is the way we enforce low-rank w.r.t. $\mathbf{X}$ and the use of self-similarity. In addition, we are interested in colummnwise sparsity of $\mathbf{S}$, whereas in robust PCA, the sparsity regards any element of $\mathbf{S}$.

For hyperspectral images, an usual assumtions is that the columns (spectral vectors) of matrix $\mathbf{X}$ live in a low-dimensional subspace that may be estimated from the observed data $\mathbf{Y}$ with good approximation [2, 7]. Thus, we write $\mathbf{X} = \mathbf{E}\mathbf{Z}$ [2], with $\mathbf{E} \in \mathbb{R}^{n_b \times p}$ and $p \ll n_b$, and $\mathbf{E}$ holding an orthogonal basis for the signal subspace. Hence, the observation model (1) may be written as

$$\mathbf{Y} = \mathbf{E}\mathbf{Z} + \mathbf{S} + \mathbf{N}. \tag{2}$$

C. Denoising

Based on the observation model (2), we propose to estimate matrix $\mathbf{Z}$ and the sparse matrix $\mathbf{S}$ representing outliers. Matrices $\{\mathbf{Z}, \mathbf{S}\}$ may then be inferred by solving the optimization

$$\{\widehat{\mathbf{Z}}, \widehat{\mathbf{S}}\} \in \arg\min_{\mathbf{Z},\mathbf{S}} \frac{1}{2}||\mathbf{E}\mathbf{Z} + \mathbf{S} - \mathbf{Y}||_F^2 + \lambda_1 \phi(\mathbf{Z}) + \lambda_2 ||\mathbf{S}^T||_{2,1}, \tag{3}$$

where $||\mathbf{X}||_F^2 = \text{trace}(\mathbf{X}\mathbf{X}^T)$ is the Frobenius norm of $\mathbf{X}$. The first term on the right-hand side represents the data fidelity and accounts for i.i.d. Gaussian noise. The second term is the first regularizer expressing prior information tailored to self-similar images [2, 4, 5, 8], and the third term is the second regularizer, the mixed $\ell_{2,1}$ norm of $\mathbf{S}^T$ given by $\|\mathbf{S}^T\|_{2,1} = \sum_{i=1}^n \|\mathbf{s}_i\|_2$ ($\mathbf{s}_i$ denotes i-th column of $\mathbf{S}$), which promotes column-wise sparsity among the columns of $\mathbf{S}$ (see, e.g. [9]) since anomalies are often spatially sparse. Finally, $\lambda_1 \geq 0$ and $\lambda_2 \geq 0$ are the regularization parameters, which set the relative weight of the respective regularizers. Assuming that ϕ is a convex function, then the optimization (3) is a convex problem.

We solve the optimization (3) with CSALSA algorithm [10]. Here we use a trick of plug-and-play approach in solving the subproblem w.r.t. $\widehat{\mathbf{Z}}$ [11]. By assuming that ϕ is decoupled w.r.t. to the bands of $\mathbf{Z}$, and noting that $\mathbf{E}$ is orthogonal, then the plug-and-play step w.r.t. $\mathbf{Z}$ amounts to apply an available denoiser, such as the BM3D [4] or LRCF [5], to each band of $\mathbf{Z}$. Since the denoisers are not proximity operators, we don't have converge guarantee for the implemented variant of CSALSA. The convergence of the plug-and-play iterative procedures is currently an active area of research [11]. In our case, we have systematically observed converge provided that the augmented Lagrangian parameter is set to $\mu \gtrapprox 1$.

The research leading to these results has received funding from the European Union's Seventh Framework Programme (FP7-PEOPLE-2013-ITN) under grant agreement n°607290 SpaRTaN.

D. Anomaly detection

We propose an anomaly detector derived from the estimate of outlier matrix $\widehat{\mathbf{S}}$ in (3), i.e.,

$$r_i = \|\hat{\mathbf{s}}_i\|_2, \quad i = 1, \ldots, n \tag{4}$$

where $\hat{\mathbf{s}}_i$ is the i-th column of outlier matrix $\widehat{\mathbf{S}}$. If r_i is larger than a threshold, then the i-th pixel is detected as an anomalous pixel.

E. Experimental Results

A semi-real hyperspectral dataset (Fig. 1 (b)) is simulated by adding i.i.d Gaussian noise and anomalous pixels to Pavia University data[1].

The denoising performance of proposed approach is compared with NAILRMA [1] and FastHyDe [2]. For quantitative assessment, the signal-to-noise (SNR) index and the structural similarity (SSIM) index [2] of each band are calculated. The corresponding mean SNR (MSNR) and mean SSIM (MSSIM) are reported in Table I. The quality of reconstruction may also be inferred from Fig. 2. We can see that proposed method is able to preserve anomaly pixels in denoised results. Meanwhile, proposed anomaly detector is compared with the state-of-the-art anomaly detectors, namely global RX [12], local RX [12], OSP global RX [13], OSP local RX [13], NRS [14], and BSJSBD [15] (Fig. 3).

TABLE I
QUANTITATIVE ASSESSMENT OF DIFFERENT DENOISING ALGORITHMS APPLIED TO SEMI-SYNTHETIC DATASET.

Index	Noisy Image	NAILRMA	FastHyDe	Proposed
MSNR (dB)	20.31	33.25	38.13	**38.58**
MSSIM	0.8295	0.9949	0.9982	**0.9983**
Time (Seconds)	-	480	**25**	213
MSNR (dB)	25.65	36.86	42.24	**43.16**
MSSIM	0.9303	0.9972	0.9991	**0.9992**
Time (Seconds)	-	477	**25**	214
MSNR (dB)	30.84	40.64	47.58	**49.34**
MSSIM	0.9697	0.9987	**0.9997**	**0.9997**
Time (Seconds)	-	488	**25**	218
MSNR (dB)	35.40	44.49	47.36	**51.11**
MSSIM	0.9910	0.9995	0.9998	**0.9999**
Time (Seconds)	-	482	**26**	220
MSNR (dB)	40.19	47.81	49.56	**54.27**
MSSIM	0.9964	0.9997	**0.9999**	**0.9999**
Time (Seconds)	-	475	**26**	222

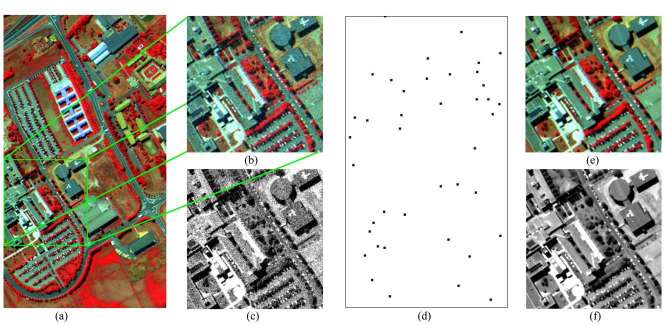

Fig. 1. (a) Clean Pavia University scene (b) A subset of simulated noisy image (20.31 dB) with 0.02 percentage of outliers (c) A subset of noisy image (Band 61) (d) Groundtruth of outliers (e) A subset of denoised image by proposed approach. (f) A subset of denoised image by proposed approach (Band 61).

[1]Pavia scenes were provided by Prof. Paolo Gamba from the Telecommunications and Remote Sensing Laboratory, Pavia university (Italy) and can be downloaded from http://www.ehu.eus/ccwintco/index.php?title=Hyperspectral_Remote_Sensing_Scenes.

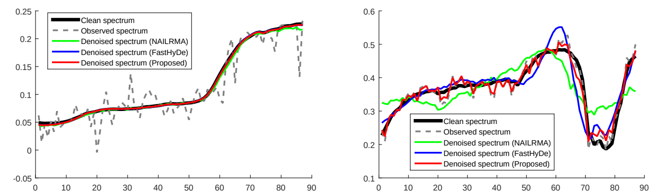

Fig. 2. Denoised spectral signatures of a normal pixel (left) and denoised spectral signatures of a anomaly pixel (right) in simulated noisy data (20.31 dB) with 0.02 percentage of outliers. Note that the noise in anomaly pixel is not removed completely since our main objective w.r.t. anomalies is to keep them rather than to denoise them and our output result is $\widehat{\mathbf{Z}} + \widehat{\mathbf{S}}$.

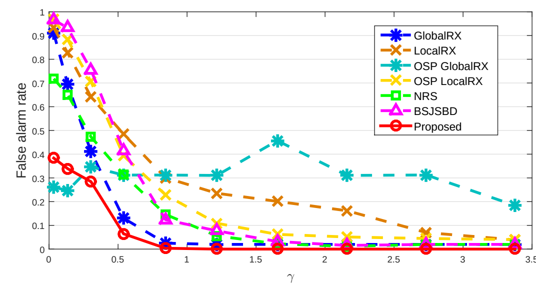

Fig. 3. False alarm rate as a function of the relative power of the rare pixels that lies orthogonal complement of the signal subspace, denoted ad γ, for SNR = 20.31dB. As γ decreases, the detection of the outliers becomes more difficult. The false alarm rate is calculated as the ratio between the number of background pixels wrongly categorized as targets and the total number of detected pixels when all targets have been detected.

II. Conclusion

We have proposed a new denoising method with preservation of rare pixels. As an extension of FastHyDe [2], the new method exploits three characteristics of HSIs: a) low-rank, b) self-similarity, and c) column-wise sparsity of outlier matrix. A comparison with the state-of-the-art algorithms is conducted, leading to the conclusion that proposed denoising approach yields better performance for additive noise with preservation of rare pixels. The derived anomaly detector shows superior detection performance.

References

[1] W. He, H. Zhang, L. Zhang, and H. Shen, "Hyperspectral image denoising via noise-adjusted iterative low-rank matrix approximation," *IEEE Journal of Selected Topics in Applied Earth Observations and Remote Sensing*, vol. 8, no. 6, pp. 3050–3061, 2015.

[2] L. Zhuang and J. Bioucas-Dias, "Fast hyperspectral image denoising based on low rank and sparse representations," in *2016 IEEE International Geoscience and Remote Sensing Symposium (IGARSS 2016)*, 2016.

[3] S. Matteoli, M. Diani, and G. Corsini, "A tutorial overview of anomaly detection in hyperspectral images," *IEEE Aerospace and Electronic Systems Magazine*, vol. 25, no. 7, pp. 5–28, Jul. 2010.

[4] K. Dabov, A. Foi, V. Katkovnik, and K. Egiazarian, "Image denoising by sparse 3-d transform-domain collaborative filtering," *IEEE Transactions on Image Processing*, vol. 16, no. 8, pp. 2080–2095, Aug. 2007.

[5] M. Nejati, S. Samavi, S. Soroushmehr, and K. Najarian, "Low-rank regularized collaborative filtering for image denoising," in *Image Processing (ICIP), 2015 IEEE International Conference on*. IEEE, 2015, pp. 730–734.

[6] J. Wright, A. Ganesh, S. Rao, Y. Peng, and Y. Ma, "Robust principal component analysis: Exact recovery of corrupted low-rank matrices via convex optimization," in *Advances in neural information processing systems*, 2009, pp. 2080–2088.

[7] J. Bioucas-Dias, A. Plaza, N. Dobigeon, M. Parente, Q. Du, P. Gader, and J. Chanussot, "Hyperspectral unmixing overview: Geometrical, statistical, and sparse regression-based approaches," *IEEE Journal of Selected Topics in Applied Earth Observations and Remote Sensing*, vol. 5, no. 2, pp. 354–379, Apr. 2012.

[8] A. Buades, B-Coll, and J-M Morel, "A non-local algorithm for image denoising," in *2005 IEEE Computer Society Conference on Computer Vision and Pattern Recognition (CVPR'05)*. IEEE, 2005, vol. 2, pp. 60–65.

[9] J. A. Tropp, A. C. Gilbert, and M. J. Strauss, "Algorithms for simultaneous sparse approximation. Part I: Greedy pursuit," *Signal Processing*, vol. 86, no. 3, pp. 572–588, 2006.

[10] M. Afonso, J. Bioucas-Dias, and M. Figueiredo, "Fast image recovery using variable splitting and constrained optimization," *IEEE Transactions on Image Processing*, vol. 19, no. 9, pp. 2345–2356, 2010.

[11] S. V. Venkatakrishnan, C. A. Bouman, and B. Wohlberg, "Plug-and-play priors for model based reconstruction," in *2013 IEEE Global Conference on Signal and Information Processing*, Dec. 2013, pp. 945–948.

[12] I. S. Reed and X. Yu, "Adaptive multiple-band cfar detection of an optical pattern with unknown spectral distribution," *IEEE Transactions on Acoustics, Speech, and Signal Processing*, vol. 38, no. 10, pp. 1760–1770, Oct. 1990.

[13] L. Ma and J. Tian, "Anomaly detection for hyperspectral images based on improved rx algorithm," in *International Symposium on Multispectral Image Processing and Pattern Recognition*. International Society for Optics and Photonics, 2007, pp. 67870Q–67870Q.

[14] W. Li and Q. Du, "Collaborative representation for hyperspectral anomaly detection," *IEEE Transactions on Geoscience and Remote Sensing*, vol. 53, no. 3, pp. 1463–1474, March 2015.

[15] J. Li, H. Zhang, L. Zhang, and L. Ma, "Hyperspectral anomaly detection by the use of background joint sparse representation," *IEEE Journal of Selected Topics in Applied Earth Observations and Remote Sensing*, vol. 8, no. 6, pp. 2523–2533, Jun. 2015.